Electronic Supplementary Information (ESI) for

Asymmetric nickel hollow fibres as the catalytic membrane reactor for CO_2 hydrogenation into syngas

Mingming Wang[a], Xiaoyao Tan[a,*], Xiaobin Wang[b], Bo Meng[b] and Shaomin Liu[c]

1. Experimental details

1.1 Preparation of the asymmetric Ni hollow fibers

The Ni hollow fibers were fabricated by a modified spinning-sintering technique [1]. A spinning slurry was firstly prepared by dispersing the Ni powder uniformly in the polysulfone (PSf) solution with N-methyl-2-pyrrolidone (NMP) as the solvent. The composition of the spinning slurry was 62.25 wt% Ni powder, 12.5 wt% PSf, and 25 wt% NMP. After degassing, the spinning solution was pressurized with 0.15 MPa N_2 gas through a spinneret with the orifice/needle tube diameter of 3.0/1.5 mm into a tap water, using a 90wt% NMP aqueous solution as the bore liquid, to form hollow fibre precursors. The hollow fiber precursors were sintered at 1200 °C for 3 h under a 50 mol% H_2-N_2 atmosphere to form dense metallic membranes.

1.2 H_2 permeation and RWGS reaction measurement

The H_2 permeation property and the RWGS reaction performance of the Ni hollow fibers were measured using a membrane module schematically described elsewhere [2]. The Ni hollow fibers were connected to two quartz tubes on both ends, where a high-temperature silicone sealant that is able to withstand up to 350 °C was used to seal the joints. It was then housed in a Φ10×400 mm quartz tube with two PTFE vessel covers on both ends. A tubular furnace of 23 cm in overall length was used for heating so that the sealing points were kept out of the hot zone of the furnace. The effective heating length of the furnace was 5 cm. For H_2 permeation measurement, a H_2-He mixture was fed into the shell side while N_2 as the sweep gas was passed co-currently through the lumen side to collect the permeated hydrogen. The gas feed flow rates were controlled with the gas mass flow controllers. A soap bubble flow meter was used to measure the flow rates of the permeate and the retentate gas. Gas compositions were

measured online using a gas chromatograph (Agilent 6890N) fitted with a 5 Å molecular sieve column (3 mm diameter and 3 m length) and a TCD detector. High-purity Ar with the flow rate of 20 cm^3 min^{-1} was used as the carrier gas. The overall H_2 permeation flux was calculated by Eq. (1),

$$J^{e}_{H_2,\ overall} = \frac{F_{in}(x_f - x_e)}{A_m(1 - x_e)} \tag{1}$$

or

$$J^{e}_{H_2,\ overall} = \frac{F_{out} y_e}{A_m} \tag{2}$$

where F_s, F_{in} and F_{out} are flow rates of the H_2-He mixture, the CO_2 feed and the syngas product, respectively; A_m is the membrane permeation area calculated by $A_m = \pi(D_o - D_{in})L/\ln(D_o/D_{in})$, in which D_o, D_{in} and L are the outer diameter, inner diameter and the effective fiber length for H_2 permeation, respectively; x_f and x_e are the H_2 concentrations (mol%) in the feed and the retentate, respectively; and y_e is the CO_2 or the CO concentration (%) in the syngas stream.

For the RWGS reaction experiment, CO_2 instead of N_2 as the sweep gas was introduced into the fiber lumen. A cold trap was used to condense the water vapor of the product gas before entering the GC. The CO_2 conversion was calculated by,

$$X_{CO_2} = \left(1 - \frac{F_{out} y_{CO_2}}{F_{in}}\right) \times 100\% \tag{3}$$

where y is the CO_2 or the CO concentration (%) in the syngas stream.

1.3 Characterization

Morphology and microstructure of the hollow fiber membranes were observed with scanning electron microscopy (SEM) on HITACHI S-4800 (Japan). The gas-tight property of the hollow fiber membranes was confirmed by the nitrogen gas permeation test at room temperature [3]. The porosity of the hollow fibers was measured by the Archimedes method with distilled water as the liquid medium. The samples were immersed in the distilled water tank with ultrasonic for 5 min so that all the open pores were filled with water. The porosity was calculated according

to $\varepsilon = 1 - \rho_{App} / \rho_{XRD}$, where ρ_{App} is the measured apparent density of the Ni hollow fibers and ρ_{XRD} is the theoretical density of the metallic nickel. The N_2 adsorption-desorption isotherms of the hollow fiber were measured in the pressure range up to 1 atm at 77 K. Before measurements, every sample was degassed at 383 K for 6 h under vacuum.

References

[1] X. Tan, N. Liu and B. Meng, J Membr Sci, 2011 ,**378**, 308.

[2] M. Wang, J. Song and X. Wu, J Membr Sci, 2016 ,**509**, 156.

[3] X. Tan, Y. Liu and K. Li, AIChE J, 2005,**51**,1991.

2. Model of the hydrogen permeation through asymmetric Ni hollow fiber membrane

Considering that the H_2 partial pressures on both the shell and the lumen sides vary along the hollow fiber due to the permeation, the permeability of the asymmetric hollow fiber membranes has to be analyzed with the permeation model related to local permeation flux. Figure S1 shows the flowing pattern for H_2 permeation in the asymmetric hollow fiber. A model is established as follows to describe the permeation process based on the assumptions: 1) isothermal and isobaric operation. 2) plug flow for both the feed and the sweep gas; 4) negligible external mass transfer resistance; 5) ideal gas behavior.

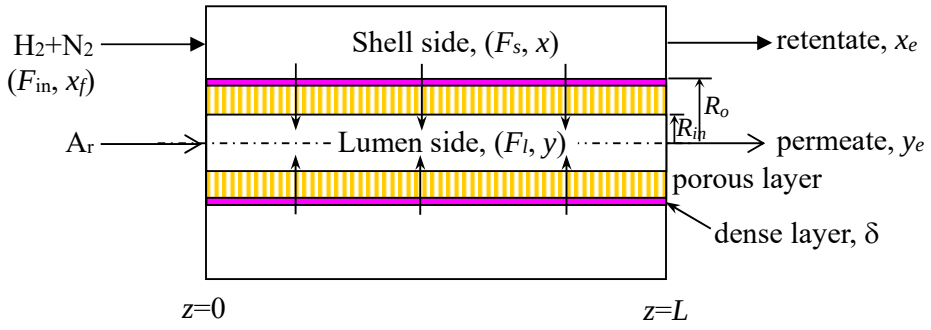

Figure S1 Flowing pattern of the H_2 permeation in the asymmetric hollow fiber membrane

The mass conservation equations for the shell and the lumen gas phases can be written as,

H_2 in shell side: $\frac{d}{dz}(F_s x) = -2\pi R_m \cdot J_{H_2}$ (4)

N_2 in shell side: $F_s(1-x) = F_{in}(1-x_f)$ (5)

H_2 in lumen side: $\frac{d}{dz}(F_l y) = 2\pi R_m \cdot J_{H_2}$ (6)

Ar in lumen side: $F_l(1-y) = F_{Ar}$ (7)

The boundary conditions for Eqs (4-5) are given by,

$z = 0, \quad x = x_f, \quad y = 0$ (8)

In the above governing equations, F_s and F_l (mol s^{-1}) are the molar flow rate of the shell and lumen phase, respectively; x and y are the molar fraction of H_2 in the shell and lumen phase; R_m is the logarithmic mean radius of the hollow fiber calculated by $R_m = \frac{R_o - R_{in}}{\ln(R_o / R_{in})}$; F_{in} and F_{Ar} (mol s^{-1}) are the feed flow rates of the H_2-N_2 mixture and the Ar sweep gas, respectively. The local H_2 permeation flux in mol m^{-2} s^{-1} can be expressed by the Sieverts' equation [8],

$J_{H_2} = Q \cdot \left((p_a x)^{0.5} - (p_a y)^{0.5} \right)$ (9)

where p_a is the atmospheric pressure (1.013×10^5 Pa), and Q is the H_2 permeance through the membrane (mol m^{-2} s^{-1} $Pa^{-0.5}$), which is a function of temperature and membrane thickness expressed by,

$Q = \frac{P_{H0} \exp(-E_a / RT)}{\delta}$ (10)

where P_{H0} is the pre-exponential factor of H_2 permeability (mol m^{-1} s^{-1} $Pa^{-0.5}$); E_a the activation energy (J mol^{-1}); R the ideal gas constant (8.314 J mol^{-1} K^{-1}), T the permeation temperature (K), and δ is the effective membrane thickness (m).

3. SEM images of the Ni hollow fiber precursor

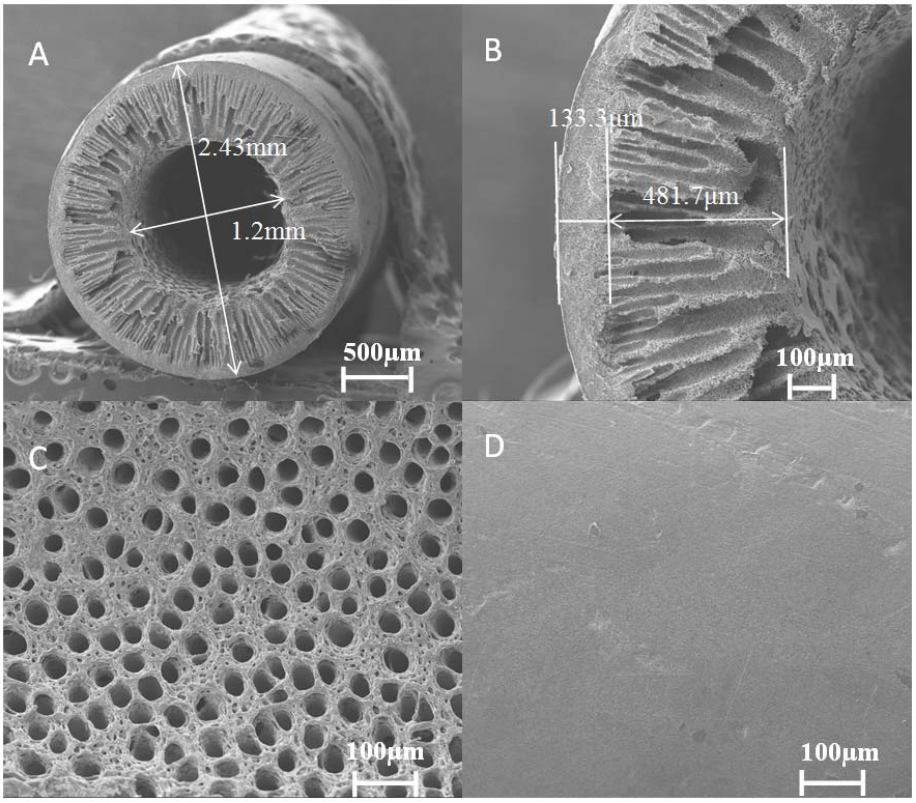

Figure S2 SEM images of the Ni hollow fiber precursor: A-cross section; B-wall; C-inside surface; D-outside surface

4. The Arrhenius plot of the H_2 permeance of the hollow fibre

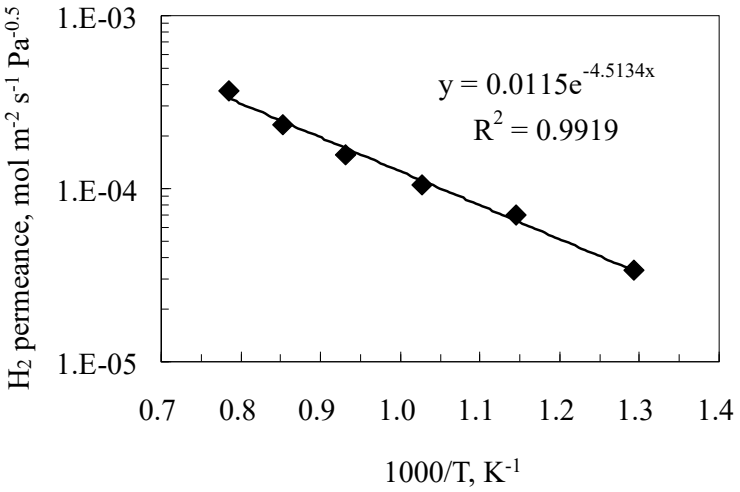

Figure S3 Arrhenius plot of the H_2 permeance of the asymmetric hollow fiber against temperature

5. Effects of CO_2 flow rate

At higher gas flow rates, the contact time of gases with the membrane reactor would be shortened, significantly influencing the RWGS. The effect of the sweep gas on the membrane reactor performance during the RWGS reaction was investigated. Fig.S4 shows the H_2 flux, CO_2 conversion, CO yield, and syngas composition as a function of temperature under different CO_2 feed flow rate. The feed flow rate of 50% H_2-N_2 mixture was fixed at 2.23×10^{-5} mol s^{-1}. Figure S4 (a) shows the H_2 permeation flux as a function of temperatures at different CO_2 sweeping rate. Just as expected, the H_2 permeation flux increased with increasing the temperature and CO_2 sweeping rate. Higher CO_2 flowrates consume more H_2 thus expanding the driving force for H_2 permeation. It is quite logic to observe that CO_2 conversion and CO yield decreased with the sweep gas flow rate increment at a given temperature (Figure S4(b)) as the residence time deceases with the higher gas hourly space velocity (GHSV). For example, at 1000 ^oC, as the CO_2 sweeping rate decreased from 3.35×10^{-5} to 1.12×10^{-5} $mols^{-1}$, the CO yield increased from 20.53% to 38.21% and the CO_2 conversion increased from 23.11% to 39.63%. Given the experimental error range, the carbon is well balanced before and after going through the hollow fiber. Fig. S4(c) presents the H_2 and CO concentrations in the CO_2 sweep side as a function of CO_2 flow rate. It is clearly seen that both H_2 and CO concentrations increased with decreasing the CO_2 flow rate and H_2 concentration is lower than CO concentration.

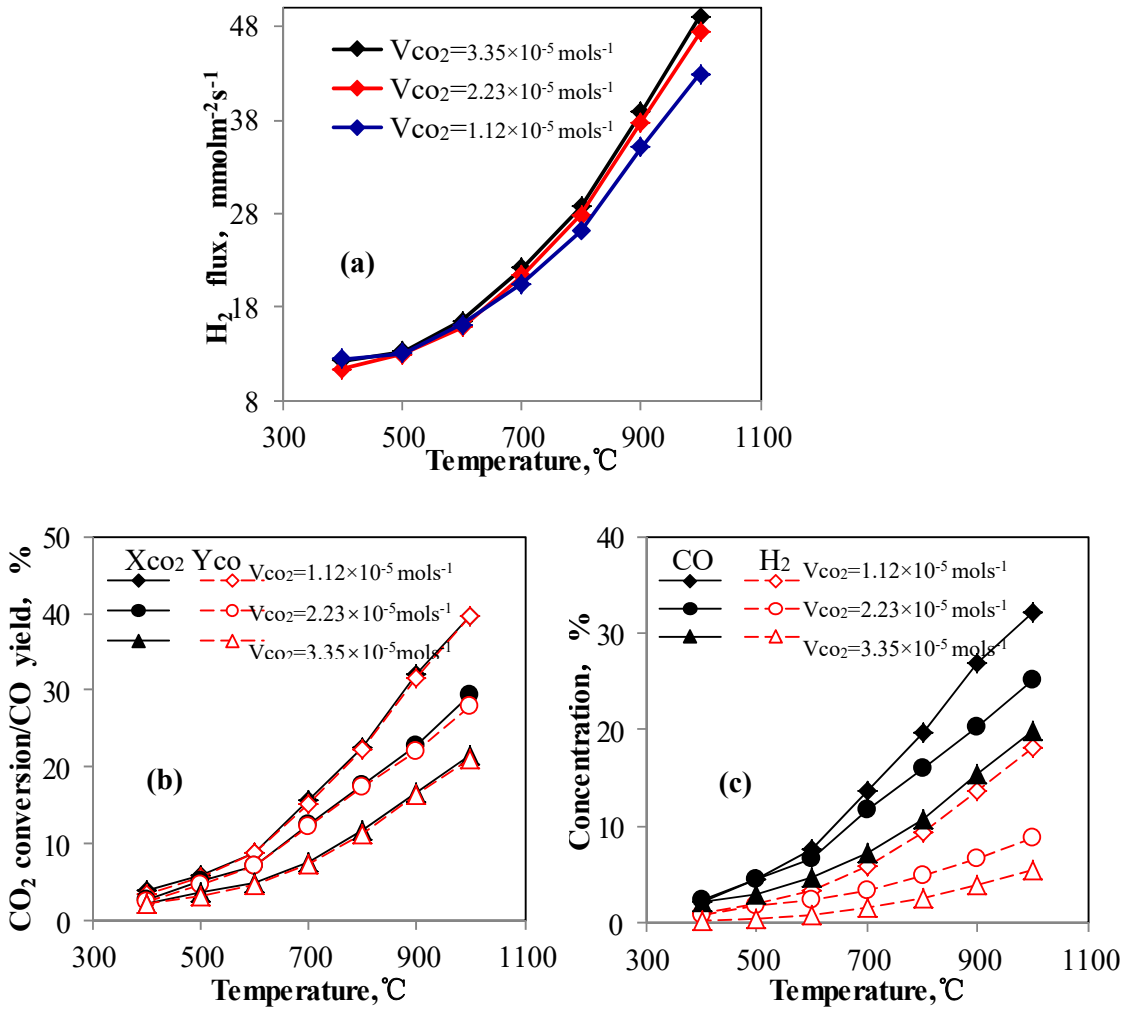

Figure S4 Effects of CO_2 flow rate on (a) H_2 flux; (b) CO_2 conversion and CO yield and (c) H_2 and CO concentrations in sweep side as a function of temperature (H_2-N_2 feed flow rate: 2.23×10^{-5} mol·s^{-1}).

6. Stability test of the Ni hollow fiber membrane

The stability of the Ni hollow fiber membrane was tested for 80 h at 900 °C using 50% H_2 as feed and CO_2 as the sweep gas. The CO_2 conversion and H_2 permeation rate were shown in Figure S5(a). It can be seen that the CO_2 conversion and H_2 permeation rate remained stable during the reaction test of 80 hours, the Ni hollow fibre showing a good thermal stability and resistance to carbon deposition. Figure S5(b) shows the inner surface of the hollow fibre after the reaction and permeation test. It is well known that Ni-based catalysts have a high

thermodynamic potential for coke formation. However, no obvious coke formation was observed on the membrane inner surface (reaction side) and inside the pores (Fig. S5(b1-b2)) after long term stability test. The carbon balances of the feed gas before and after the permeation tests between 500-1000°C were performed to evaluate the possible carbon deposition on the membrane surface. We found that the calculated difference of the overall carbon content from CO and CO_2 in the effluent from the feed was only between 0.11-2%. Given the experimental error range, the carbon is well balanced before and after going through the hollow fiber.

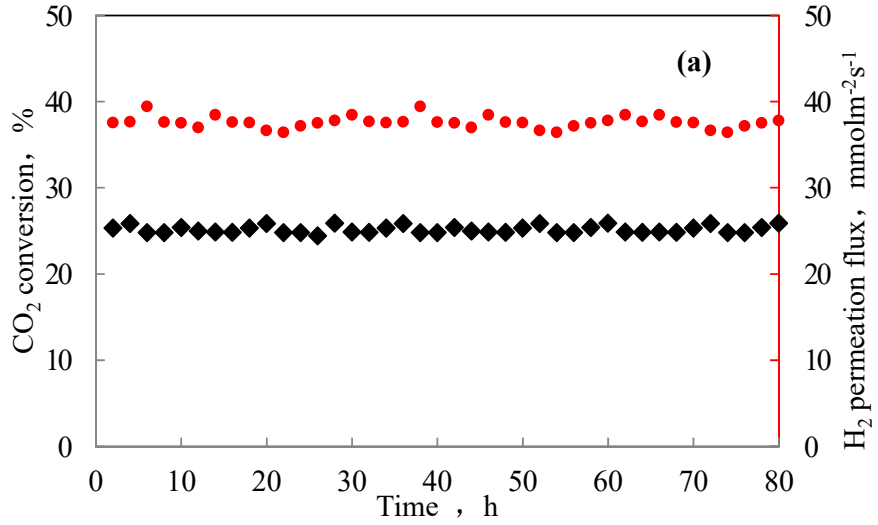

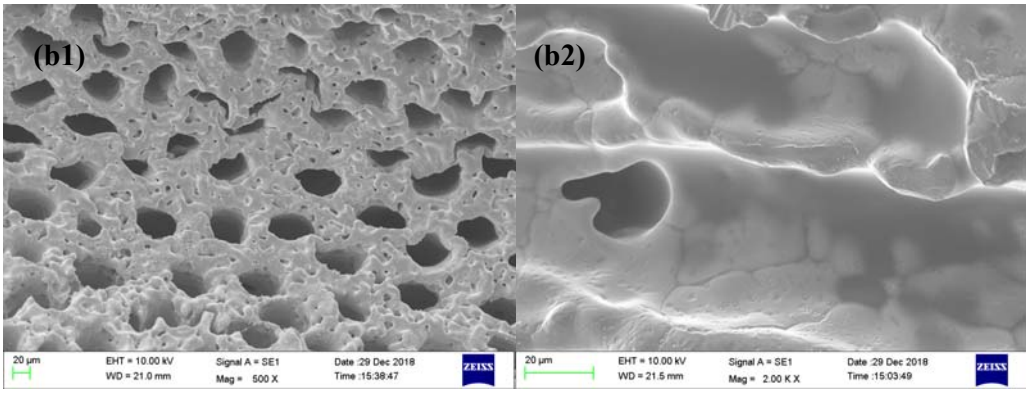

Figure S5 (a) CO_2 conversion and H_2 permeation flux for 80-hour test at 900 °C (H_2-N_2 feed flow rate of 2.23×10^{-5} mol s^{-1}; CO_2 feed flow rate of $.24\times1\ 0^{-5}$ mol·s^{-1}) **(b)** SEM images of the inner surface (feed side) (b1-inner surface; b2-finger hole) after the long term test.